Title: Ancient introgression explains mitochondrial genome capture and mitonuclear discordance among South American collared *Tropidurus* lizards

Running title: Ancient introgression and discordance in lizards

Matheus M. A. Salles[1*], André L. G. Carvalho[2], Adam D. Leaché[2], Nicolas Martinez[3], Frederick Bauer[3], Martha Motte[3], Viviana Espínola[3], Miguel T. Rodrigues[4], Carla Piantoni[5], Marcio R. Pie[1], André Olivotto[1], Guarino R. Colli[6], Erik L. Choueri[7], Fernanda P. Werneck[7], Fabricius M. C. B. Domingos[1]

[1] Programa de Pós-graduação em Zoologia, Universidade Federal do Paraná, Curitiba/PR, Brasil

[2] Department of Biology & Burke Museum of Natural History and Culture, University of Washington, Seattle/WA, USA

[3] Museo Nacional de Historia Natural del Paraguay, Asuncion, Paraguay

[4] Instituto de Biociências da Universidade de São Paulo, São Paulo/SP, Brasil

[5] School of Life Sciences, University of Hawaii at Manoa, Honolulu/HI, USA

[6] Departamento de Zoologia, Universidade de Brasília, Brasília/DF, Brasil

[7] Programa de Coleções Científicas Biológicas, Coordenação de Biodiversidade, Instituto Nacional de Pesquisas da Amazônia, Manaus/AM, Brasil

[*]*Author for Correspondence*: Matheus Salles, Programa de Pós-Graduação em Zoologia, Universidade Federal do Paraná (Departamento de Zoologia, Setor de Ciências Biológicas, Centro Politécnico, Avenida Cel. Francisco H Santos, Jardim das Américas, 81531-980, Curitiba/PR, Brasil), matheus.salles@ufpr.br.

Data availability

The data underlying this article, including phylogenetic datasets, corresponding trees, input and output files for all analyses, and any other relevant supplementary files are available in Zenodo, at https://doi.org/10.5281/zenodo.15376373.

Author contributions

Matheus Salles: study design, analyses, lead writing. Fabricius Domingos and André Carvalho: study design, field sampling, genome sequencing, writing final draft. Nicolas Martinez, Frederick Bauer, Martha Motte, Viviana Espínola, Miguel T. Rodrigues, Carla Piantoni, Guarino R. Colli, Fernanda P. Werneck: field sampling efforts and/or provision of collection materials and infrastructure. Márcio Pie, André Olivotto, Erik Choueri, Adam Leache: lab work, genome sequencing. All authors read, commented and approved the final draft of the manuscript.

Acknowledgments

We thank all the institutions that provided technical, material, and structural support during the sampling phase of this study, namely the Herpetological Collection of the University of Brasília (CHUNB), the Amphibians and Reptiles Collection of the National Institute of Amazonian Research (INPA-H), the Biosciences Institute of the University of São Paulo (IB-USP), the American Museum of Natural History (AMNH), the Museo Nacional de Historia Natural del Paraguay (MNHNP), the Mato Grosso Federal University (UFMT), Museo de Historia Natural Alcide d'Orbigny, and the Universidade Nacional de Salta (UNSa). We extend our gratitude to our esteemed colleagues Eliana Lizarraga, Felipe F. Curcio (UFMT), Karina Atkinson and Jean-Paul Brouard (Fundación Para La Tierra, Paraguay), Johanna López, Nestor Romero (and family) (Estancia Cerrados del Tagatiya), Pastor Enmanuel Pérez-Estigarribia (and

family), Ricardo Céspedes, Rodrigo Ayala, and Rolando Rivas for crucial assistance or support during fieldwork. We thank Angela Coda for allowing access to the Reserva Natural Cerrados del Tagatiya and Malvina Duarte for allowing access to the Reserva Natural Laguna Blanca. We also thank Junior Nadaline and Carlos Daniel Rivadeneira for their invaluable assistance with genetic sample processing and DNA sequencing. MTR also thanks all members of his lab for help in the field. Finally, we extend our gratitude to Prof. Renato Pires Machado (UFPR) for his valuable contributions throughout the corresponding author's PhD project.

Funding

This work was funded by the Brazilian National Council for Scientific and Technological Development (CNPq #200798/2010-3), the São Paulo Research Foundation (FAPESP #2011/50146-6, #2016/08249-6, #2017/20235-3), the U.S. National Science Foundation [NSF #1855845], the Explorers Club, the Andrew Sabin Family Foundation, the American Museum of Natural History (Richard Gilder Graduate School), and the Brazilian funding agency 'Coordenação de Aperfeiçoamento de Pessoal de Nível Superior' (CAPES), which provided a PhD scholarship to the correspondent author. FPW thanks CNPq for a productivity fellowship (#307695/2023-9).

Conflict of Interest

The authors declare no conflicts of interest.

Benefit-Sharing Statement

A research collaboration was developed with scientists from the countries providing genetic samples, all collaborators are included as co-authors, the results of research have been shared

with the broader scientific community, and the research addresses a priority concern, in this case the evolutionary history of organisms being studied. More broadly, our group is committed to international scientific partnerships, as well as institutional capacity building.

Abstract

Mitonuclear discordance—evolutionary discrepancies between mitochondrial and nuclear DNA phylogenies—can arise from various factors, including introgression, incomplete lineage sorting, recent or ancient demographic fluctuations, sex-biased dispersal asymmetries, among others. Understanding this phenomenon is crucial for accurately reconstructing evolutionary histories, as failing to account for discordance can lead to misinterpretations of species boundaries, phylogenetic relationships, and historical biogeographic patterns. In this study, we investigate the evolutionary drivers of mitonuclear discordance in the *Tropidurus spinulosus* species group, which contains nine species of lizards inhabiting open tropical and subtropical environments in South America. Using a combination of population genetic and phylogenomic approaches, applied to mitochondrial and nuclear data, we identified different instances of gene flow that occurred in ancestral lineages of extant species. Our results point to a complex evolutionary history marked by prolonged isolation between species, demographic fluctuations, and potential episodes of secondary contact with genetic admixture. These conditions likely facilitated mitochondrial genome capture while diluting signals of nuclear introgression. Furthermore, we found no strong evidence supporting incomplete lineage sorting or natural selection as primary drivers of the observed mitonuclear discordance. Therefore, the unveiled patterns are most consistent with neutral demographic processes, coupled with ancient mitochondrial introgression, as the main factors underlying the mismatch between nuclear and mitochondrial phylogenies in this system. Future research could further explore the role of other demographic processes, such as asymmetric sex-biased dispersal, in shaping these complex evolutionary patterns.

Keywords: Introgression; Mitogenome; Molecular Evolution; Phylogenomics; Squamata.

Introduction

Mitochondrial and nuclear genomes evolve independently, through distinct processes, often leading to conflicting genetic patterns—a phenomenon known as mitonuclear discordance. Cases of mitonuclear discordance are increasingly reported across a wide range of animal species. Recent examples can be found among mammals (Good et al. 2015; Phuong et al. 2016; Seixas et al. 2018; Fedorov et al. 2022), birds (Andersen et al. 2021; DeRaad et al. 2023), reptiles (Firneno et al. 2021), amphibians (Zieliński et al. 2013; Dufresnes et al. 2020; Rancilhac et al. 2021), and insects (Hinojosa et al. 2019; Dong et al., 2023). Generally, conflicting patterns between nuDNA and mtDNA arise from processes such as introgression, demographic fluctuations, sex-biased dispersal asymmetries, incomplete lineage sorting (ILS), human introductions, or *Wolbachia* infection in insects (see reviews by Toews and Brelsford 2012; Bonnet et al. 2017; Deprés 2019). Determining whether mitonuclear discordance is driven by any of these factors requires a clear understanding of the genealogies among different loci, the demographic history of populations, and their historical introgression/migration patterns and rates. Notably, these complexities often present significant empirical challenges in resolving the underlying causes of discordance.

Most cases of discordance are attributed to mtDNA introgression (Toews and Brelsford 2012) and are generally associated with processes such as gene flow across hybrid zones (Zieliński et al. 2013; Good et al. 2015; Dufresnes et al. 2020; Mao and Rossiter 2020) and mitochondrial capture (Andersen et al. 2021). The latter refers specifically to a form of complete introgression, where the mitochondrial genome of one species is entirely replaced by another's (Zieliński et al. 2013). Mitochondrial capture can occur at various stages of the speciation process and between distantly related species (Rancilhac et al. 2021). Additionally, mitochondrial introgression can take place with minimal or not accompanying nuDNA

introgression (Zieliński et al. 2013; Good et al. 2015; Andersen et al. 2021; Rancilhac et al. 2021; Fedorov et al. 2022), making it challenging to detect introgressed nuclear and mitochondrial markers simultaneously (Bonnet et al. 2017; Seixas et al. 2018). Therefore, ILS is another phenomenon that cannot be overlooked in discussion of mitonuclear discordance, given the challenges in distinguishing it from introgression (Andersen et al. 2021; DeRaad et al. 2023). While some studies have identified ILS as a primary driver of mitonuclear discordance, these remain relatively rare (e.g., Firneno et al. 2021).

Demographic factors, such as fluctuation in population sizes, particularly at the periphery of a species' geographic range, can also contribute to mitonuclear discordance (Phuong et al. 2016; Dufresnes et al. 2020; Fedorov et al. 2022). In this scenario, neutral processes such as genetic drift can help in the fixation of mtDNA haplotypes at range edges of expanding populations (Bonnet et al. 2017). Even in situations where introgression involves both mtDNA and nuclear loci, mtDNA is expected to reach fixation faster, since it has a smaller effective population size and is non-recombining (Moore 1995). Following demographic expansions and secondary contact, nuclear genomes can fully recombine, thereby diluting historical introgression signals, whereas divergent, non-recombining mitochondrial haplotypes may persist.

Finally, selection can also play a role in generating mitonuclear discordance (Toews and Brelsford 2012). If a beneficial mitochondrial mutation arises but is initially incompatible with the nuclear genetic background of a population, selection may favor nuclear variants that restore mitonuclear compatibility. This compensatory selection could lead to a scenario where the advantageous mitochondrial mutation spreads widely, while the nuclear DNA follows a different evolutionary trajectory. Empirical evidence robustly demonstrates that natural selection can drive mtDNA introgression between populations through hybridization, even in

the absence of corresponding nuDNA introgression, provided there is even a minor selective advantage (Excoffier et al. 2009; Zieliński et al. 2013; Good et al. 2015; Phuong et al. 2016). As a result, the mitochondrial genome with the highest fitness may introgress into another species, regardless of whether it originates from the resident or the invading population.

Here, we investigate the drivers of mitonuclear discordance in a biological system with known occurrences of this phenomenon, the lizard family Tropiduridae (e.g., *Microlophus*: Benavides et al. 2007; 2009; *Tropidurus*: Carvalho et al. 2016). Specifically, we explored the evolutionary history of nine lineages within the *T. spinulosus* group using a multi-locus genomic approach. This diverse group of lizards is distributed across open-vegetation tropical and subtropical environments in South America and predominantly inhabit rocky and arboreal habitats (Frost et al. 1998; Carvalho 2013, 2016; Carvalho et al. 2013). Although the taxonomy of the *Tropidurus spinulosus* group has been relatively stable, new species continue to be described (e.g., Carvalho 2016). Additionally, our research includes all taxa presently admitted for the group plus one undescribed species, which is currently undergoing formal description (Carvalho et al. in prep) and is referred to as *Tropidurus sp. nov.* in this study.

We integrated mitochondrial genomes, nuclear ultraconserved elements (UCEs), and single nucleotide polymorphisms (SNPs) derived from UCEs to assess whether the mitochondrial genealogy corresponded to reciprocally monophyletic nuclear lineages. To determine the potential sources of the mitonuclear discordance, we examine the relative contributions of neutral and selective processes. Specifically, we first compared mtDNA and nuclear phylogenies to identify conflicts and potential introgression patterns, using methods that either account for ILS or do not. In a scenario where these approaches yield largely congruent results, this would suggest that ILS may not play a major role in the observed mitonuclear discordance. Second, we evaluated whether mtDNA introgression was

accompanied by detectable levels of nuDNA introgression, as most cases of discordance are attributed to processes such as gene flow across hybrid zones. We also assessed signals of positive selection on mtDNA to evaluate potential adaptive processes in shaping mitonuclear discordance. Finally, as demographic processes can contribute to emerging phylogenetic discordant patterns as well, we examined historical changes in population size to assess their role in shaping the observed discordance, as this would align with expectations under a non-adaptive scenario.

Methods

Sampling and Lab work

The phylogenomic approaches used in this study were based on anchored sequencing methods, specifically Ultraconserved Elements (UCE) as described by Faircloth et al. (2012). We sequenced a total of 43 individuals (Supplementary Material, Table S9), representing all species of the *Tropidurus spinulosus* group. RAPiD Genomics LLC (Gainesville, FL) was tasked with sample library preparation and target enrichment of UCEs using the tetrapod 5k probe set (Faircloth et al. 2012), followed by multiplexed paired-end (PE) sequencing (2 × 100 bp) of UCEs on an Illumina HiSeq 3000 PE100 platform. Our samples are mainly distributed around the Pantanal Basin, with some extending to dry environments of Paraguay and Argentina (Figure 1).

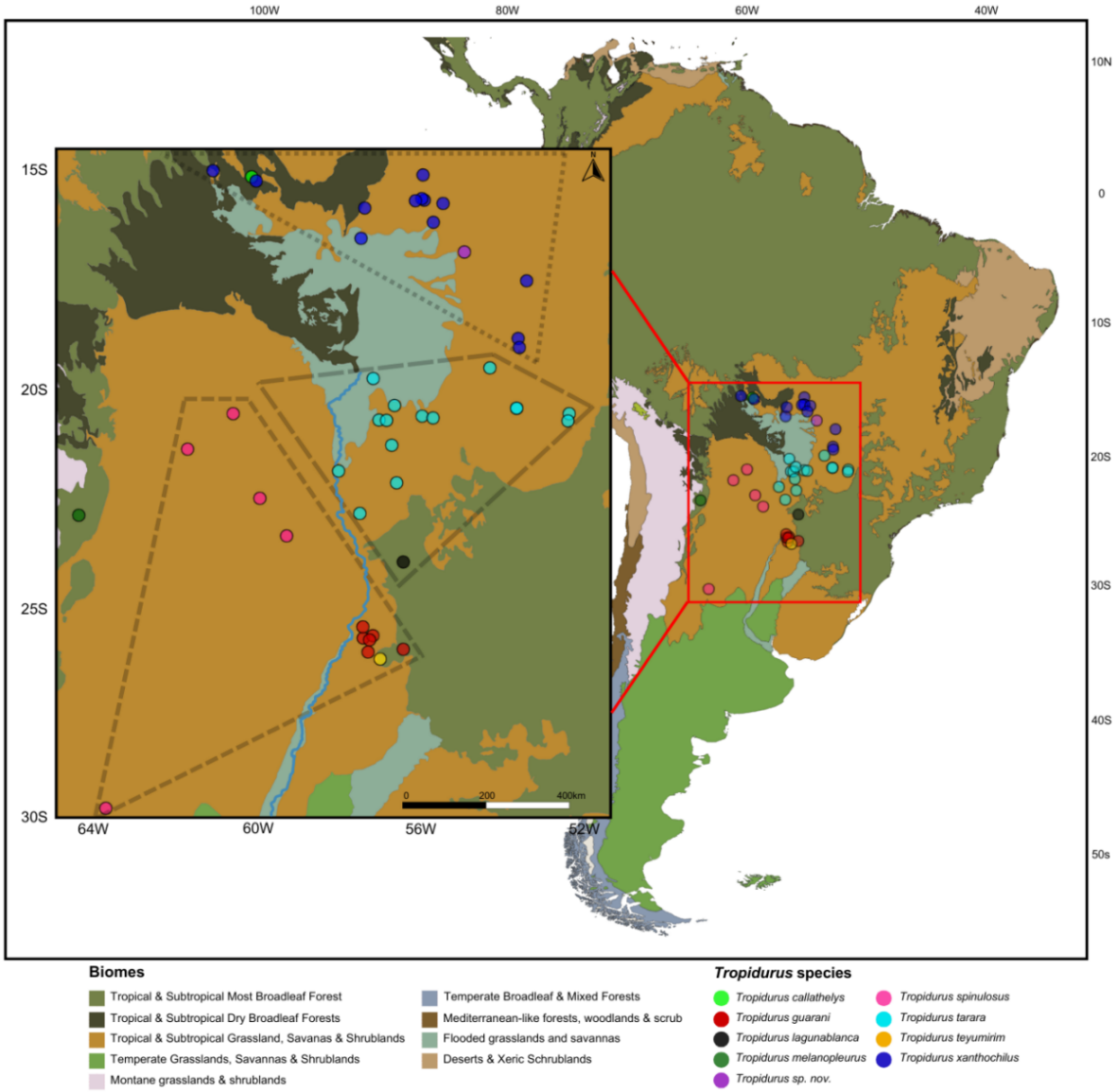

Figure 1. Sample distribution with species assignments based on our concatenated phylogenetic analysis. The map at a larger scale shows the distribution of samples across various South American biomes, according to the classification of "Terrestrial Ecoregions of the World" adopted by the World Wildlife Fund. For a detailed review of the resolution and delimitation differences in these ecoregions, see Olson et al. (2001). The smaller-scale map highlights the specific region where the analyzed samples are distributed. Phylogenetically identified groups are marked with three distinct dashed line patterns, emphasizing their allopatric distribution: (1) the *T. spinulosus* + *T. guarani* + *T. teyumirim clade* (multi-species), (2) the *T. tarara clade* (with *T. lagunablanca* tentatively considered a synonym of *T. tarara*), and (3) the *T. xanthochilus* + *T. sp. nov.* clade. The map on the smaller box also shows part of the course of the Paraguay River (light blue), which separates the *T. spinulosus* lineages to the west from *T. guarani* and *T. tarara* to the east.

UCEs and mtDNA pipeline

We assembled the reads using the Phyluce v1.7.1 pipeline (Faircloth 2016). Demultiplexed reads were cleaned to remove low quality bases and adapter sequences in Trimmomatic (Bolger et al. 2014), using the wrapper program illumiprocessor in Phyluce. To

accelerate assembly and render difficult datasets tractable, we normalized read depth at a minimum of 5 using the script bbnorm.sh available in the BBTools suite (Bushnell 2018). Trimmed and normalized reads were inspected for quality and adapter contamination using FastQC v0.11.9 (Andrews 2010), and then assembled into contigs with SPAdes v3.15.5 (Bankevich et al. 2012). We used Phyluce to align assembled contigs back to their associated UCE loci, remove duplicate matches, create a taxon-specific database of contig-to-UCE matches and extract UCE loci for all individuals. Specifically, contigs matching UCE loci were identified and extracted using the program LastZ v1.0 (Harris 2007) within Phyluce, both in incomplete and complete (75% and 95% of completeness) matrices (see Faircloth 2016). After probes and UCEs were matched, we aligned UCE contigs with MAFFT v7.471 (Katoh and Standley 2013) using specific customized settings (-globalpair, --maxiterate 1000, --adjustdirection), and trimmed the resulting alignments using the internal-trimming algorithm (Gblocks: Castresana 2000). As a final step, AMAS (Borowiec 2016) was used to compute final summary statistics for all alignments.

Due to the high abundance of mtDNA in samples and the less-than-perfect efficiency of target enrichment methods, mitochondrial data, including entire mitogenomes are often generated as a byproduct of the UCE sequencing process (Allio et al. 2020). Thus, we extracted mtDNA from our contig assembly produced through Phyluce using MitoFinder (Allio et al. 2020), which can find and extract multiple mitochondrial genes or even entire mitogenomes from assembled sets of bulk sequences. In general terms, the same alignment process described above for UCEs was adopted for mitochondrial data.

SNP calling workflow

We selected the sample with the largest number of UCE loci among all individuals ('MTR 29586', with 4800 loci) retrieved during the extraction step described above as the main reference during the process of calling single nucleotide polymorphisms (SNPs), as recommended in the Zarza et. al. (2016) pipeline to extract SNPs from UCE reads. Then, we followed the sequence capture data from population-level samples workflow developed by Harvey et al. (2016). The first step involves BWA, which was used to map raw reads from individuals to contigs (Li et al. 2009; Li 2013). Thus, SAM files were converted to BAM with SAMtools (Li et al. 2009). Alignments were checked for BAM format violations, read group header information was added, and PCR duplicates were marked for each individual using Picard (v. 1.106). The resulting BAM files for each individual in a lineage were merged into a single file with Picard, which was then indexed with SAMtools. The Genome Analysis Toolkit (GATK; v. 3.4-0; McKenna et al. 2010) was used to locate and realign around indels, which was followed by calling SNPs using the 'UnifiedGenotyper' tool in GATK. SNPs and indels were then annotated and indels were masked. Finally, we used GATK to restrict our datasets to high-quality SNPs (Q30 filter) and performed read-backed phasing. After that, we used the R packages SNPfiltR (DeRaad 2022) and vcfR (Knaus and Grunwald 2017) to visual and iteratively filter our SNP dataset based on specific quality and completeness metrics. For analyses requiring unlinked SNPs, a linkage disequilibrium-based filtering approach was applied using PLINK (Purcell et al. 2007) with fixed parameters (--indep-pairwise 50 10 0.5). At the end of this process, two datasets were generated. The first, referred to as the '*unlinked SNP dataset I*', included 42 samples and excluded the *Tropidurus melanopleurus* sample, retaining only one sample external to the largest clade within the group, namely *T. callathelys* (used in D-suite analysis; 40,265 SNPs, 25.34% missing data). The second one, '*unlinked SNP dataset II',* with

37 samples, excluding the *T. melanopleurus, T. callathelys, T. teyumirim* and *T. sp. nov.* samples, and assigning the *T. lagunablanca* sample as *T. tarara* (used in Stairway Plot analysis; 27,454 SNPs, 24.71 % missing data).

Gene and species tree analysis

Gene trees for all UCE loci and the mtDNA locus were inferred using IQ-TREE v2.2.6 (Minh et al. 2020), and support was inferred using 1000 ultrafast bootstraps (≥ 95 considered as strong support). For partitioned ML analyses, ModelFinder (Kalyaanamoorthy et al. 2017), part of the IQ-TREE package, was used to select the best fit model for each partition followed by tree reconstruction (-m TESTNEWMERGE option), allowing partitions to have different evolutionary rates (-spp option). Support was inferred using 1000 ultrafast bootstraps. Additionally, species trees were inferred for the UCE dataset using ASTRAL v5.15.4 (Zhang et al. 2018), which does this from gene trees and provides internal branch lengths in coalescent units of gene tree discordance, as well as branch support values in the form of local posterior probabilities (LPPs). In our ASTRAL analyses, we used the topology resulting from the partitioned approach produced through IQ-TREE as a reference. Finally, we used BPP v.4.6 (Flouri et al., 2018) to estimate a species tree for the *Tropidurus spinulosus* group, based on the full dataset of 820 UCE loci.

In the case of mitochondrial data, besides partitioning by gene, the alignment was also partitioned by third codon positions (in the case of coding sequences), and we did an additional analysis including two outgroup species to evaluate the monophyly of the *Tropidurus spinulosus* group — *Plica plica* and *T. torquatus* (Figure S6; GenBank accession numbers: AB218961 for *P. plica*, and KU245273, KU245300, KU245090 and KU245062 for *T. torquatus*). We present only the trees (both based on nuDNA and mtDNA) featuring species

from the *T. spinulosus* group (our in-group) in the results section. In all cases, trees were manually rooted in *T. melanopleurus* using FigTree (Rambaut 2014), following the topology obtained in the previously described analysis.

Divergence time estimation

A time-tree was inferred using two different approaches. The first one was the RelTime-Branch Lengths method (Tamura et al. 2018), available in MEGA11 (Tamura et al. 2021), which uses a phylogenetic tree previously estimated branch lengths to infer divergence dates. In this case, the time-tree was computed using the UCE-based phylogenetic tree (complete matrix) with one calibration constraint, namely the node separating *Tropidurus callathelys* from all the other species in the group (and using *T. melanopleurus* as the outgroup). We used 10.74 Ma as the reference value for this constraint following the estimates obtained by Zheng and Wiens (2016) regarding the node separating *T. callathelys* and the rest of the species in our ingroup. The method described in Tao et al. (2020) was used to estimate confidence intervals and set a normal distribution on the node for which calibration densities were provided, and a normal distribution was used with the mean centered on 10.74 and standard deviation = 0.5.

Alternatively, divergence time estimates were also estimated using the MCMCTree v4.10 program (dos Reis and Yang 2019), which uses an approximate likelihood calculation approach. In this case, the 100 most clocklike UCE loci within our dataset were selected, particularly the loci with the least root-to-tip variance. Clock-likeness was assessed using the program SortaDate (Smith et al. 2018), which measures root-to-tip variance within gene trees and then sorts them from highest to lowest variance. The calibration in this case was performed by constraining the age of the same node described above by > 10 and < 11 Ma,

using a fixed topology. Molecular clock estimates were obtained using the independent rates model and we used the HKY85 model. The gamma prior on the mean substitution rate for partitions (rgene_gamma) was set to G (7, 9.75), which means a substitution rate of approximately 0.00717 substitutions/site/Ma (value available for the phylogenetically closest species to *Tropidurus* in the germline mutation rate study of Bergeron et al. 2023). The gamma rate variance (sigma2_gamma) was specified with G (1, 10). Two independent runs were performed, each consisting of 550.000 MCMC iterations, with 10.000 as burn-in, 'nsample' = 100.000, and 'sampfreq' = 5. The ESS of the MCMCTree runs were examined in Tracer v.1.7 (Rambaut et al. 2018) to determine convergence, and values > 200 were retained.

Gene flow and phylogenetic network estimation

Failing to consider the potential influence of gene flow and introgressive hybridization among species can negatively impact phylogenetic inference (e.g. Solís-Lemus and Ané 2016; Solís-Lemus et al. 2016). Therefore, given the mitonuclear discordance observed in the *Tropidurus spinulosus* clade, we evaluated the potential for reticulate evolution in our dataset using five different approaches: (i) the phylogenetic networks applying quartets (SNaQ) method implemented in PhyloNetworks (Solís-Lemus and Ané 2016; Solís-Lemus et al. 2017); (ii) the maximum pseudolikelihood estimate (MPL) method implemented in PhyloNet (Wen et al. 2018); (iii) the extension of the typical tree-based model to general networks, assuming no ILS and independent loci, available in the NetRAX program (Lutteropp et al. 2022); (iv) ABBA-BABA tests for detecting gene flow between pairs of species, through the D-suite program (Malinsky et al., 2021); and (v) the MSC-M model implemented in BPP v.4.6 (Flouri et al. 2018; 2023) to estimate migration rate between pair of species that showed signals of mitonuclear discordance. The first four methods serve as exploratory tools to identify potential

reticulations or gene flow events, while the BPP-based approach directly quantifies migration rates. Regarding the network and the ABBA-BABA approaches, please refer to the Supplementary Material, section "*Details on phylogenetic networks methodology and results*," for a detailed explanation on all reticulation tests.

To directly assess how gene flow differentially impacted nuclear and mitochondrial genomes, we used the migration model (MSC-M) available in BPP v.4.6 (Flouri et al. 2018; 2023). This allowed us to estimate the number of migrants per generation and the direction of gene flow for species showing the strongest mitonuclear discordance in our phylogenetic trees. This was done in two stages, either using the nuclear species tree or the mitochondrial genealogy as the guide tree. In the first case, we used only a portion of the nuDNA dataset—specifically, the 100 most clocklike UCEs selected using SortaDate (Smith et al. 2018). A second migration analysis was performed using that same dataset, but this time incorporating mitochondrial data alongside nuclear data. In other words, two analyses were conducted using the nuclear topology as the guide tree: one using nuclear markers only (100 UCE loci, 93,246 bp) and another combining nuclear data with mitochondrial data (100 UCE loci, 93,246 bp + 1 mitochondrial partition, 13,578 bp).

In both cases we tested bidirectional migration scenarios with the following species: *Tropidurus xantochilus* ↔ *T. guarani*, *T. xanthochilus* ↔ *T. spinulosus,* and *T. xanthochilus* ↔ *T. tarara*. Scenarios involving ancestral populations or species of the following groups were also tested. For analyses using the mitochondrial genealogy as the guide tree, these included: (A) *T. tarara* and one *T. xanthochilus* group; (B) *T. guarani* and *T. spinulosus*; (C) *T. guarani, T. spinulosus* and another *T. xanthochilus* group. When using the nuclear topology as the guide tree, the same scenarios with current species mentioned above were tested, while also considering the following scenarios involving ancestral nodes: (B) *T. guarani* and *T. spinulosus*;

(D) *T. sp. nov.* and *T. xanthochilus*; (E) *T. tarara, T. guarani*, *T. spinulosus* and *T. teyumirim*; (F) *T. guarani*, *T. spinulosus* and *T. teyumirim.* Population sizes (θ) were also estimated and recorded for each species and ancestral node involved in the migration pairs. In all cases, we used an inverse gamma prior of G(3, 0.04) for the Θ parameter and G(3, 0.2) for the τ parameter, fixing the species model prior on the topologies described above. The gamma migration prior used was 0.1 (α = 1, β = 10). We ran analyses for 4 x 10^5 MCMC generations, taking samples every five and using 5 x 10^3 burn-in generations. To check for consistency of results, we conducted two independent runs for each analysis.

Furthermore, we also used POPART v. 1.7 (Leigh et al. 2015) to generate a TCS haplotype network (Clement et al. 2002), based on 3 mitochondrial genes - cytochrome c oxidase I, II, and III (COX1, COX2, and COX3).

Tests for positive selection and demographic changes through time

To detect significant deviations from the hypothesis of neutral evolution in the mtDNA dataset, we tested for the evidence of positive selection using MEME (Mixed Effects Model of Evolution; Murrell et al. 2012), BUSTED (Branch-Site Unrestricted Statistical Test for Episodic Diversification; Murrell et al. 2015), aBSREL (adaptive Branch-Site Random Effects Likelihood; Smith et al. 2015), and FUBAR (Fast, Unconstrained, Bayesian Approximation; Murrell et al. 2013). MEME is designed to identify sites underlying episodic selection, BUSTED provides a gene-wide (not site-specific) test for positive selection by asking whether a gene has experienced positive selection at least one site on at least one branch, aBSREL focuses on tree branches and can be used to test if positive selection has occurred on a proportion of branches, while FUBAR uses a Bayesian approach to infer nonsynonymous (dN) and synonymous (dS) substitution rates on a per-site basis for a given coding alignment and

corresponding phylogeny. All of these tests were performed utilizing the HYPHY package through the DataMonkey server, using default parameters, and the threshold of $p < 0.05$ for all four analyses. The same alignment of mitochondrial genes used for the phylogenetic analyses was utilized here, with the particularity that in order to perform the selection analyses, stop codons of each coding gene were removed, manually. Besides, Tajima's D was calculated to evaluate evidence of natural selection and population size changes in the mitogenome using the R function 'tajima.test', from the 'pegas' package (Paradis 2010). Mitochondrial nucleotide diversity was estimated for populations of *T. guarani*, *T. spinulosus*, *T. tarara*, and *T. xanthochilus* using the 'nuc.div' function, also from the 'pegas' package.

Because selection tests indicated neutrality in the mtDNA dataset (see results), we then performed the multilocus coalescent-based Extended Bayesian Skyline Plots (EBSP; Heled and Drummond 2008) implemented in BEAST v2.7.6 (Bouckaert et al. 2019) to estimate changes in effective population sizes over time. Four phylogenetic groups were used in this analysis, namely: *Tropidurus guarani*, *T. spinulosus*, one *T. tarara* clade and *T. xanthochilus*. Regarding this, we highlight that demographic analyses typically assume that each analyzed group is monophyletic and below the species level. While *T. guarani* is consistently recovered as paraphyletic in our nuclear phylogenies, it forms a monophyletic clade sister to *T. spinulosus* in mitochondrial analyses. Therefore, for the EBSP analysis, which was performed exclusively with mitochondrial data, *T. guarani* was treated as a single lineage. A similar issue arises with *T. tarara*, which appears as two distinct mitochondrial groups. In this case, analyses were conducted separately for each cluster, but since the results were identical, only one is presented in the text, as it effectively represents both *T. tarara* groupings. In the remaining cases, samples were divided according to the clades recovered in the mtDNA partitioned approaches previously described.

To reduce computational burden and facilitate convergence, we conducted separate analyses on three sets of mitochondrial genes rather than using the entire mitochondrial genome. These sets included: 1) cytochrome b (cytb); 2) COX1, COX2, and COX3; 3) 12S and 16S ribosomal RNAs. For coding gene analyses, alignments were partitioned by gene and codon position, with tree and clock models linked across all partitions. Site models were treated independently, with BEAST Model Test performed separately for each partition to estimate mutation rates, and restricting potential models to the "namedExtended" set. Regarding substitution rates, we set 1.0×10^{-2} as the mean for the COX partition, 6.339×10^{-3} for the 12s + 16s partition, and 1.94×10^{-2} for the cytb partition, all reference values already used in previous studies which used similar approaches when dealing with *Tropidurus'* mtDNA in BEAST (e.g., Werneck et al. 2015; Camurugi et al. 2022; Carvalho et al. 2024). An uncorrelated relaxed molecular clock was adopted in all three cases (with a normal distribution for the 'ucldMean'; Sigma = 0.0025). Because the default of the hyper-prior of the mean of the population size distribution ("populationMean.alltrees") is a sensitive option and takes a long time to converge (requiring longer runs), we modified the prior to a Normal distribution centered on 1.0 (Mean) with a standard deviation of 0.1 (Sigma) to improve convergence. Initial tests were carried out to determine the optimum number of MCMC simulations required for each of the populations. In most tests, we ran 500,000,000 MCMC simulations, sampled every 50,000 chains. In all cases, three independent runs were carried out and we checked for convergence using Tracer 1.7 (Rambaut et al. 2018) by visually checking effective sample size (ESS > 200). In specific cases where convergence was not achieved with this number of simulations, we combined logs with LogCombiner (Rambaut and Drummond 2014) and used those files to generate EBSP plots.

To infer the demographic history using the nuDNA dataset, we first generated a folded SFS file for the SNP dataset with easySFS (Gutenkunst et al. 2009). We then used Stairway Plot v. 2.18 (Liu and Fu 2020) to estimate historical effective population size changes of *Tropidurus xanthochilus*, *T. tarara*, *T. spinulosus* and *T. guarani*. For this last group, only the 4 samples that form a clade in the partitioned phylogenetic analyses described above were used (Figures S1-S6). The parameters for the Stairway Plot analysis were as follows: 67% for the training sites, and one year was assumed as generation time (A. Carvalho, pers. commun.). The nuclear mutation rate was assumed to be 7.17×10^{-9} substitutions/site/generation, which is the value available for the phylogenetically closest species to *Tropidurus* in the germline mutation rate study of Bergeron et al. (2023).

Table 1 provides a summary of all analyses conducted in this study, along with their respective objectives and main results.

Table 1. Overview of the analytical workflow used in this study, detailing the rationale behind each step. SNP = single nucleotide polymorphism; MSA = multiple sequence alignment; nuc = nuclear; mt = mitochondrial.

Method	Data	Analysis	Objectives	Main results
IQ-TREE	MSA-nuc (100, 95 and 75% UCE matrices) MSA-mt (coding + non-coding regions)	Individual-level phylogenies	What are the phylogenetic relationships of sampled individuals? Do nuc and mt topologies agree?	nuc: Three main clades detected: (*Tropidurus xanthochilus* + *T. sp. nov.*), (*T. tarara* + *T. lagunablanca*), (*T. teyumirim* + *T. guarani* + *T. spinulosus*), in addition to *T. melanopleurus* and *T. callathelys* as external lineages to the clade comprising all those species. mt: Strong disagreement between mitochondrial and nuclear-based phylogenies.
ASTRAL	MSA-nuc (100, 95 and 75% UCE matrices)	Species-level phylogenies	Does the species tree agree with the relationships inferred in the individual-level phylogenies?	Overall, it agrees with the IQ-TREE nuclear phylogenies.
BPP	MSA-nuc (100% matrix)	Species tree		
RelTime-Branch Lengths	Nuclear phylogenetic tree (100% UCE complete matrix)	Divergence times	When did the diversification of the *T. spinulosus* group	Major divergence events occurring from 20 Ma onward. The initial split

MCMCTree	MSA-nuc (100 most clocklike UCE loci selected through SortaDate)		occur? Could this temporal pattern be linked to the species' demographic history, or might it help explain gene flow events throughout their evolution?	occurred between 20 and 15 Ma, with *T. melanopleurus* diverging first. Around 10 Ma, *T. callathelys* separated from the remaining taxa, while most subsequent speciation events took place between 7.5 and 2.5 Ma.
PhyloNetworks (SNaQ)	Unrooted nuclear gene trees (100% UCE complete matrix) + concordance factors	Phylogenetic Network	Can we detect introgression in the nuclear genome? Is evolutionary history better explained by networks or bifurcating trees in this case?	All phylogenetic network results suggest minimal or no introgression within the *T. spinulosus* species group.
PhyloNet	Rooted nuclear gene trees (100% UCE complete matrix)			
NetRAX	Unrooted nuclear gene trees (100% UCE complete matrix)			
POPART (TCS haplotype network)	Three mtDNA coding genes (COX1, COX2, and COX3)	Population structure	How is mtDNA structured in the group's lineages?	The clusters align with the groupings in the mt-phylogenetic tree, exhibiting the same pattern of discordance with the nuclear data.
D-suite (ABBA-BABA tests)	SNP	Gene flow	Is gene flow occurring between species within the *Tropidurus spinulosus* group?	Minimal interspecific nuclear admixture, suggesting that introgressive hybridization has had limited impact on the nuclear genomes of these species.
BPP (MSC-M model)	MSA-nuc (100 most clocklike UCE loci selected through SortaDate) + MSA-mt (coding + non-coding regions)	Multiple parameter estimation (mainly ancestral population sizes and migration rates)	Assess how gene flow differentially impacted nuclear and mitochondrial genomes	Which phylogenetic reconstruction more accurately reflects the true history of population divergence: the nuclear species tree or the mitochondrial genealogy? In other words, is the mitochondrial genealogy a reliable representation of species history, with the nuclear tree being discordant due to factors such as incomplete lineage sorting or other processes? Or, conversely, does the nuclear tree capture the actual species relationships, while the mitochondrial genealogy is discordant due to processes like introgression or historical gene flow?
HYPHY	MSA-mt (coding regions)	Selection tests	Is there evidence of positive selection in the mitogenomes of *Tropidurus spinulosus* lineages, supporting an adaptive-based process leading to mitonuclear discordance?	Overall, there is no strong evidence of adaptive processes influencing mtDNA, with positive selection detected at only a few sites in the mitogenome.
Skyline Plot (BEAST)	MSA-mt (three partitions, comprehending six genes)	Demography tests		Demographic expansions in all analyzed species,

Stairway Plot	SNP	Estimate changes in effective population sizes over time	particularly from 70 kya onward.

Results

UCE and mtDNA phylogenomic datasets

We obtained a final dataset including 820 UCE loci for 43 individuals of nine lineages of the *Tropidurus spinulosus* species group. Our complete matrix comprised alignments with 725,505 bp after internal-trimming. Matrices with 75% and 95% of completeness generated alignments with 2,269 and 1,613 loci, 1.98M and 1.40M bp, respectively. Nuclear phylogenetic analyses using both the partitioned approach in IQ-TREE, based on complete and incomplete matrices (Figures S1-S3), and the BPP species tree approach (Figure 2), indicated that our samples can be grouped into three main clades: (*T. sp. nov. + T. xanthochilus), (T. lagunablanca + T. tarara), (T. guarani + T. spinulosus + T. teyumirim)*, in addition to *T. callathelys and T. melanopleurus* as external lineages to the clade comprising the remaining species. The trees inferred using ASTRAL, which account for ILS, produced similar patterns (Figures S4-S6). Compared to the UCE dataset, the mtDNA dataset (alignment with 40 samples, 15 genes, and 13,578 bp) produced markedly different results regarding topology, indicating a clear case of mitonuclear discordance (Figure 2; Figures S7-S8). Notably different from the nuclear trees, our mitochondrial genealogy shows that while most *T. xanthochilus* samples were grouped as sister to the clade containing *T. spinulosus* and *T. guarani*, two *T. xanthochilus* samples, the *T. sp. nov.* and the *T. teyumirim* samples, were all recovered within the *T. tarara* + *T. lagunablanca* clade. Besides, despite *T. xanthochilus* and *T. sp. nov.* forming a clade based on nuclear data, they do not appear closely related in the mitochondrial dataset. Similarly, most groups observed in these two phylogenetic trees are reflected in the haplotype network

inferred for the *T. spinulosus* group, showing the same pattern of discordance compared to the nuclear data (Figure S9).

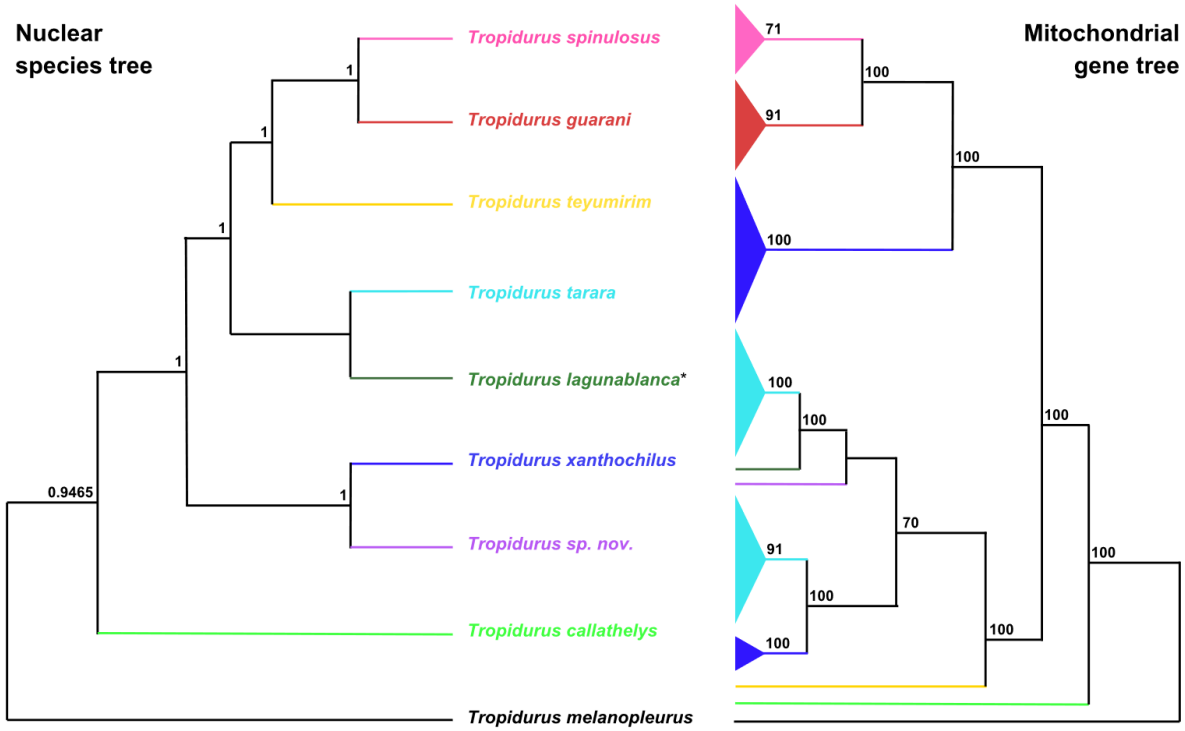

Figure 2. Comparison between the nuclear species tree and the mitochondrial gene tree for the group *Tropidurus spinulosus*. The left panel shows the species tree inferred from multilocus nuclear data using BPP, with branch support values indicated next to nodes (posterior probabilities). The right panel displays the mitochondrial gene tree inferred through IQ-TREE, with branch support shown as bootstrap values (in this case, we only show values above 70). Colored clades correspond to the same taxa in both trees. Collapsed branches in the mitochondrial tree represent intraspecific variation (for the fully detailed tree, see the Supplementary Material). *All nuclear gene trees recovered *T. lagunablanca* nested within *T. tarara* samples, indicating that these lineages likely represent a single evolutionary unit. Accordingly, the *T. lagunablanca* sample was assigned to *T. tarara* in the BPP analysis, so that they represent a single branch in the estimated species tree. However, for a clearer comparison with the mitochondrial genealogy, in this figure we present the two lineages as separate branches within the same clade.

Divergence dating with nuclear data indicates that the initial split within the *Tropidurus spinulosus* group occurred between 20 and 15 million years ago (Ma), separating *T. melanopleurus* from the other lineages. The split involving *T. callathelys* occurred approximately 10 Ma ago, and most subsequent divergence events among the remaining species of the group took place between 7.5 and 2.5 Ma (Figure 3; Figure S10). In most cases, the divergence times estimated using RelTime fall within the same 95% highest posterior

density (HPD) intervals provided by MCMCTree, but some differences can be noticed (Figures S10-11).

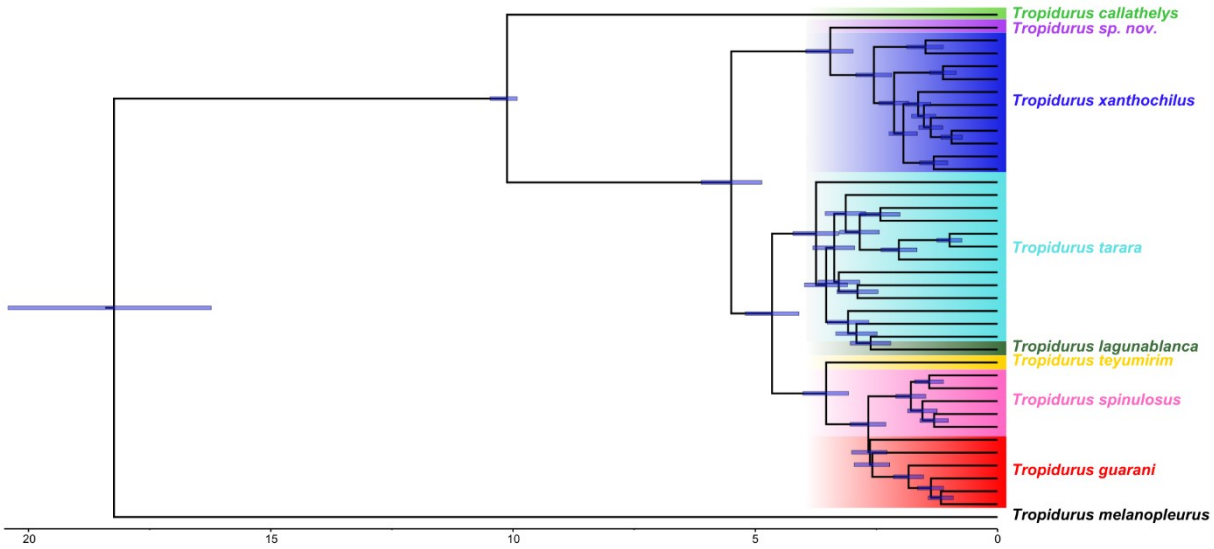

Figure 3. Divergence times (Ma) estimated for the *Tropidurus spinulosus* species group using the UCE dataset. The 95% HPD interval of the posterior estimates (blue shaded bars), as estimated through the MCMCTree program, is shown above each node of the tree. The scale bar is in Ma. Specimen names are collapsed (for the fully detailed tree, see the Supplementary Material).

Phylogenetic networks and gene flow

Analyses of the UCE dataset using PhyloNetworks revealed that models incorporating up to three reticulation events provided a better fit to our data compared to strictly bifurcating trees, where gene tree discordance is attributed solely to ILS. However, these events are mostly intraspecific and do not involve the species with discordant relationships, thus Phylonetworks does not indicate that reticulation is the main source of mitonuclear discordance (Figures S12-S15; Table S1). Analyses using the other phylogenetic network approaches corroborated the pattern of minimal reticulations between species observed in our UCE data (Figures S16-S18), and ABBA-BABA tests for detecting gene flow also do not indicate significant nuclear admixture within the *Tropidurus spinulosus* species group (Table S2). Please refer to the Supplementary Material, section "*Details on Phylogenetic Networks*

methodology and results," for a detailed explanation on all reticulation tests and respective results.

Analyses in BPP under the MSC-M model with nuclear data indicates minimal or no gene flow among extant species, but inclusion of ancestral populations yields higher migration rate estimates (Figure 4; Tables S3-S4), particularly those associated with the observed phylogenetic discordance. This pattern is robust to the choice of different guide trees: whether constrained by the mitochondrial topology or by the partitioned nuclear topology, although the first produces relatively higher migration rate values. Notably, both guide tree inferences implicate *Tropidurus xanthochilus*, or its ancestors, in these ancient gene flow events, suggesting that historical mitochondrial capture involving this lineage may underlie the main observed discordances between nuclear and mitochondrial phylogenies. Also, when combining the nuclear dataset alongside the complete mitochondrial genome, higher rate estimates were generally produced than those obtained using the nuclear dataset only. In this case, migration rates using the combined dataset (with mitochondrial and nuclear partitions) were higher than the estimates using solely the nuclear data (Table S4). In summary, across all migration scenarios evaluated, including information derived from the mitochondrial data (whether based on topology or mitogenome alignments) consistently resulted in higher inferred migration rates compared to nuclear-only analyses, demonstrating that the inclusion of mtDNA in the analysis strengthens the detection of historical gene flow in this system.

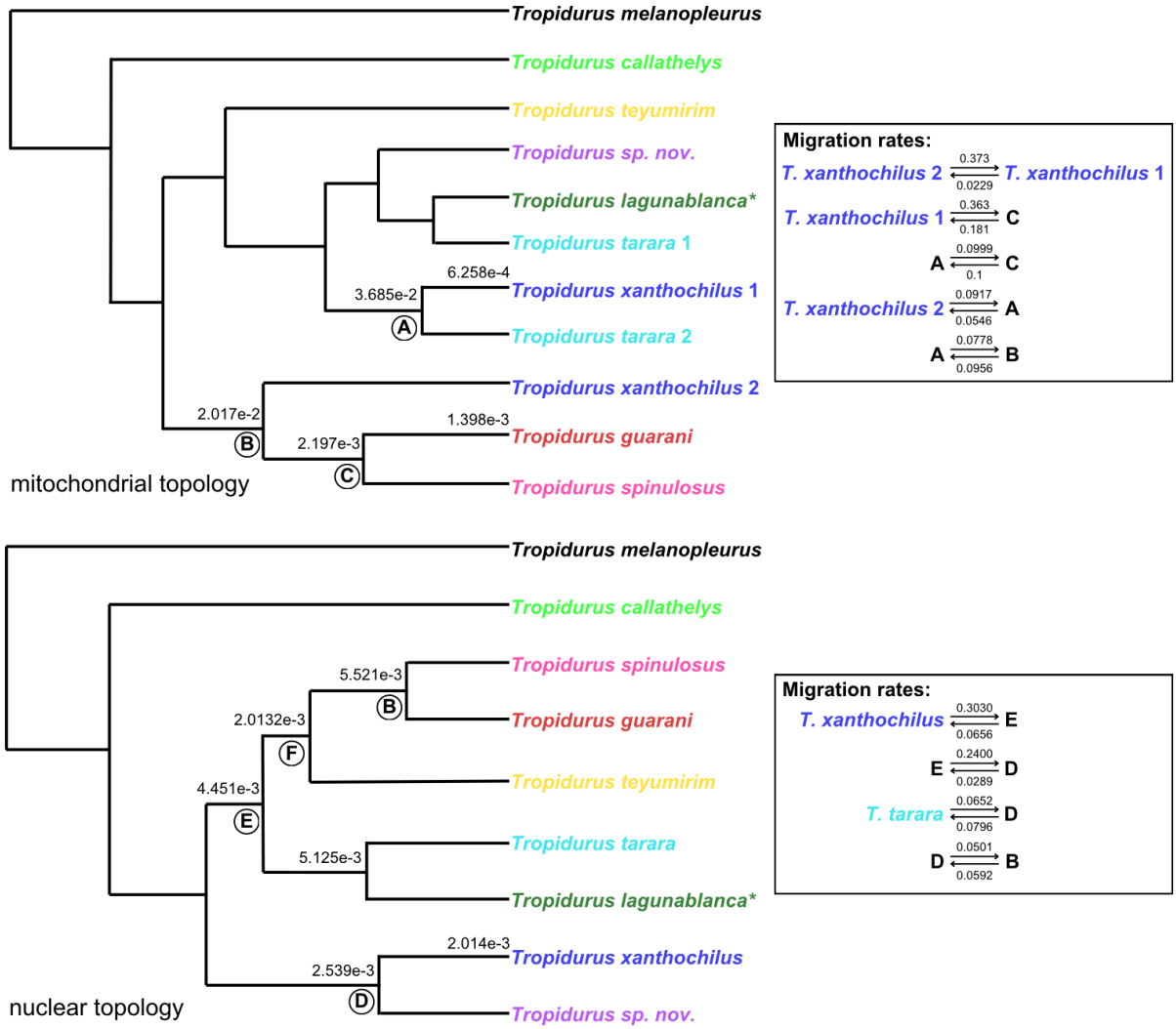

Figure 4. Migration (MSC-M) model for *Tropidurus spinulosus* species, displaying only the scenarios with the highest estimated migration rates. For a complete list of all tested migration scenarios and their corresponding rate values, please refer to the Supplementary Material. Population size (theta, θ) values for each species or ancestral node involved in gene flow events are shown above the branches, with the remaining theta values also provided in the Supplementary Material. The upper panel presents the analysis using the mitochondrial topology as the guide tree, whereas the lower panel shows the same analysis based on the nuclear topology, in this case using both nuclear and mitochondrial data as input. In both trees, the circled letters below the nodes denote the ancestral lineages included in the migration tests.

Estimates of population size (θ) for both current species and ancestral populations further support the previously described scenario (Figure 4; Tables S5-S6), for instance indicating a directional gene flow event in which the larger ancestral population of the *T. guarani* + *T. spinulosus* clade might have captured *T. xanthochilus* mitochondrial genomes.

Selection

Regarding the mtDNA dataset, our analyses indicate minimal evidence of positive selection acting on the mitogenomes of *Tropidurus spinulosus* lineages. Codon-based tests detected limited signatures of episodic positive or diversifying selection: MEME identified nine sites (two in ATP6, one in ATP8, one in COX1, two in COX2, and one in COX3) with p-values ≤ 0.05, while FUBAR detected two sites (one in COX1 and one in COX2) with posterior probabilities ≥ 0.95. In contrast, both BUSTED and aBSREL analyses did not reveal significant episodic selection along any branches in the mitogenomic phylogeny, even after formal testing of 36 branches with correction for multiple comparisons. Furthermore, we did not observe any species with extreme nucleotide diversity (π) values, which could indicate selection on mitochondrial lineages; instead, the diversity values were nearly identical across all populations (Table S7). Notably, the significantly negative Tajima's D ($p \leq 0.05$, Table S8) indicates an excess of rare variants, a pattern that can arise from both demographic expansion and selection. Subsequent analyses support a scenario of recent expansion for the main populations, suggesting that this signal is evidence of historical demographic changes rather than selection acting on the mitogenomes.

Demographic history

As previously demonstrated, BPP estimates of population size reveal differences among ancestral populations likely involved in the ancient introgression events underlying the observed discordance; these differences also support the inferred direction of gene flow (please refer to the *Migration tests in BPP* section of the Supplementary Material as well).

Furthermore, our EBSPs revealed a pronounced increase in effective population size for all populations, particularly in the last 100.000 years (Figure 5). Given that *Tropidurus*

tarara was recovered in two distinct clusters within the mitochondrial tree, we highlight that independent analyses were conducted for each group. As results were identical across both groups, we present the result for only one cluster, which we consider representative of the species as a whole. For the nuclear dataset, Stairway Plot analyses for *T. xanthochilus*, *T. tarara*, *T. spinulosus*, and *T. guarani* revealed a consistent pattern across species, characterized by population expansion mainly beginning 60,000 years ago, followed by relatively stable population sizes thereafter (Figure 6).

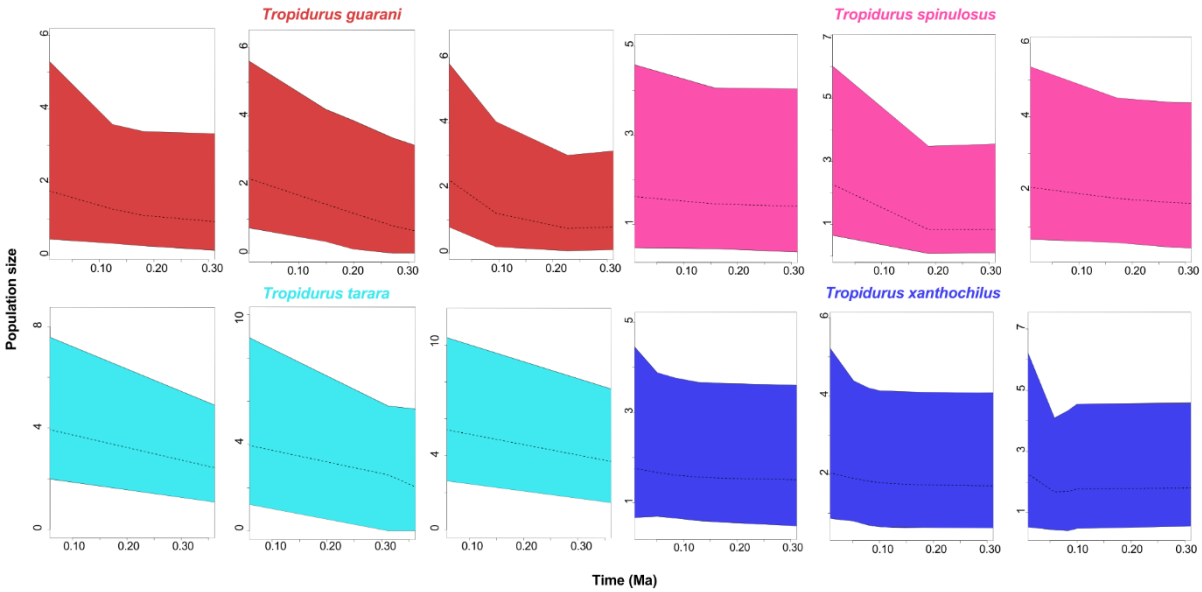

Fig. 5. EBSP results showing changes in effective population size through time for lineages in the *Tropidurus spinulosus* species group, based on three mitochondrial partitions (from left to right: cytb, 12 + 16s, and COX1, 2 and 3). Y-axis shows the effective population size with respective mean (dashed lines) and 95% HPD limits (the surrounding colored area delimited by the continuous lines). Assuming a generation time of 1 year, the current effective population size estimated at 1 would be equivalent to around 1 million. While this number appears large, it serves only as an illustration. Actual values will vary depending on the chosen mutation rate and generation time. The x-axis shows time in Ma as time goes backwards from left to right.

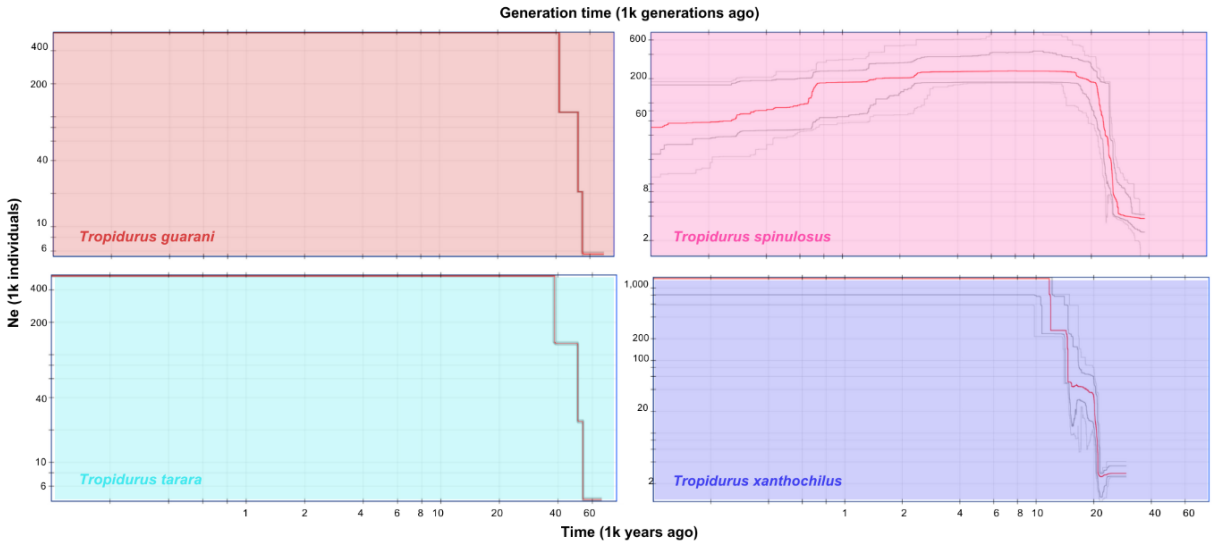

Fig. 6. Stairway Plot demographic inferences of four lineages within the *Tropidurus spinulosus* species group. The red line shows the median estimate of the effective population size (Ne). The gray lines indicate the 75% (dark) and 95% (light) confidence intervals.

Discussion

Our genomic analysis of the *Tropidurus spinulosus* species group reveals a complex evolutionary history characterized by: (a) significant discordance between nuclear and mitochondrial phylogenetic groupings, with very low levels of nuclear introgression; (b) at least two major mitochondrial capture events, specifically involving ancient *T. xanthochilus* populations and non-sister groups such as the *T. spinulosus* + *T. guarani* clade and *T. tarara*; (c) no signs of strong positive selection acting on mtDNA; and (d) demographic evidence of recent population expansions in both nuclear and mitochondrial genomes across various species in the group, along with differences in the sizes of ancestral populations that may have reinforced introgression events directionality. Given these findings, we suggest that the mitonuclear discordance observed in this study likely originated from admixture among ancient populations of the *T. spinulosus* species group that experienced long-term isolation, followed by secondary contact.

Methodological challenges in investigating introgression as a cause of mitonuclear discordance

Some caution is warranted when interpreting our results, especially given the nature of our dataset. UCEs, by definition, represent highly conserved genomic regions shared across evolutionarily distant taxa (Faircloth et al. 2012). While this might suggest that such data are primarily suited for addressing 'deep' phylogenetic questions, multiple studies have demonstrated their utility at the population and individual levels (Smith et al. 2014; Raposo do Amaral et al. 2018). Additionally, the introgression and gene flow tests we used are able to capture events on different time scales. For instance, the ABBA-BABA test assumes that multiple substitutions at a given site are rare, as an excess of substitutions can distort patterns of site discordance. This assumption tends to break down in deeply divergent taxa (Hibbins and Hahn 2022), making the ABBA-BABA test more suitable for detecting recent introgression events. In our study, only one significant case of interspecific gene flow was detected (both in the case of the PhyloNetworks analysis and the ABBA-BABA tests), though it warrants caution (as discussed below). Conversely, phylogenetic networks, which analyze discordance between gene trees and other concordant factors, are less impacted by multiple substitutions at individual sites, which makes them better suited for detecting older introgression events (Hibbins and Hahn 2022).

Therefore, as we used different methodologies capable of detecting signals across distinct time scales, our results cannot be considered totally dependent on the nature of the used markers—even considering that the accuracy of phylogenetic network methods may also depend on the number of gene trees used. In this regard, previous studies have shown that a similar number of gene trees compared to our dataset is sufficient to reliably recover an accurate network topology, although the exact direction of reticulation events may remain

uncertain depending on the evolutionary scenario (Solís-Lemus and Ané 2016). Moreover, the consistency of recovered topologies across multiple analyses, with varying levels of data completeness, suggests that the majority of our UCE gene trees are not either unresolved or phylogenetically uninformative. Therefore, although other genomic markers may offer greater sensitivity for detecting introgression, the consistency of our results across multiple analytical frameworks—each suited to detecting gene flow over different temporal scales—supports the conclusion of minimal or no nuclear introgression within the *Tropidurus spinulosus* group. In any case, future comparative studies are warranted to evaluate how the choice of genomic markers may influence the detection of complex evolutionary processes such as introgression.

Decoupled histories: mitonuclear discordance with minimal nuclear introgression

Reports of mitonuclear discordance are not unexpected, given that mitochondrial and nuclear genomes evolve semi-independently. In this context, while previous studies have documented nuclear introgression associated with mitonuclear discordance (e.g., Zieliński et al. 2013; Myers et al. 2022), our findings suggest a different pattern. For instance, while we identified one significant nuclear reticulation event involving *Tropidurus callathelys* (Figure S14) and one significant D-statistic result involving *T. teyumirim* (Table S2), these findings require cautious interpretation. First, there is no evidence suggesting contemporary hybridization within the *T. spinulosus* group. The known biology and distribution of these specific lineages do not suggest the occurrence of hybridization events between them (Carvalho et al. 2013; Carvalho 2013; 2016), although this may reflect a distinction between contemporary gene flow and the ability of our methods to detect introgression over evolutionary timescales. Second, the extreme sampling disparity (n=1 for both *T.*

teyumirim and *T. callathelys* versus larger samples for other taxa) could have contributed to false positives in ABBA-BABA tests, which have reduced sensitivity at low admixture levels (Durand et al. 2011), and PhyloNetworks analyses due to stochastic effects.

ILS is another phenomenon that can contribute to mitonuclear discordance, and its signals can easily be mistaken for those caused by introgression (Andersen et al. 2021; DeRaad et al. 2023). In our case, if some samples of a species coalesced deep in the tree, before this lineage diverged from its common ancestor, a significant portion should have coalesced if ILS were the predominant factor driving the discordance with mitochondrial data. However, even our phylogenetic network analyses explicitly accounting for ILS (particularly PhyloNetworks and PhyloNet) did not detect substantial nuclear introgression events. Moreover, the agreement between partitioned (based on IQ-TREE) and ASTRAL analyses of nuclear markers also suggests that ILS has a limited impact on the phylogenetic signal (Figures S1-S6), as ASTRAL is designed to recover the correct topology even under high levels of ILS (Zhang et al. 2018).

Finally, it is important to acknowledge the lack of methods specifically designed to detect mitochondrial genome introgression with the same level of precision available for nuclear markers. The approach adopted in this study—particularly the BPP-based framework using both mitochondrial and nuclear topologies as guide trees and integrating the mitochondrial partition with multiple nuclear loci (Figure 4)—was designed to illustrate how gene flow may differ between nuclear and mitochondrial genomes due to their distinct inheritance patterns and evolutionary dynamics. Furthermore, we also aimed at emphasizing the value of a genome-wide analytical perspective for understanding the role of introgressive hybridization in animal speciation—an approach still lacking in many biological systems (Good et al. 2015).

By doing that, we discovered that while our nuclear data largely dismiss the occurrence of prominent introgression within the *Tropidurus spinulosus* group, the mitochondrial genome presents a contrasting picture. Migration rate estimates increase when mitochondrial DNA is included—either as an additional partition or by using the mitochondrial topology as the guide tree (Tables S3-S4). Specifically, while BPP analyses of 100 UCE loci produced minimal migration rate estimates (under the nuclear-guided topology), incorporating the mitogenome into the dataset increased the estimated values despite the much larger size of the nuclear dataset. Importantly, higher migration rate estimates appeared only in scenarios involving ancestral populations (regardless of whether the nuclear or mitochondrial topology was used as the guide tree), producing more realistic values (Figure 4). These findings not only underscore the analytical value of including mitochondrial data in gene flow estimates but also support the conclusion that the nuclear phylogenies more accurately reflect species history in the *T. spinulosus* system.

Proximate explanations of mitonuclear discordance in the Tropidurus spinulosus species group

Evidence supporting a demography-related hypothesis regarding introgression typically falls into three main categories (e.g., Hinojosa et al. 2019; Palacios et al. 2023; Shen et al. 2025): (i) prolonged periods of isolation; (ii) population growth leading to secondary contact; and (iii) a biogeographic signal related to the discordance. Below, we discuss how our findings align with this framework, as the primary cause of the mitonuclear discordance reported in this study is mitochondrial capture associated with the demography of the lineages within the *Tropidurus spinulosus* group. Specifically, our results indicate ancient gene flow events occurring in populations that were likely isolated for extended periods before undergoing secondary contact, although we detected limited evidence of nuclear

introgression. Additionally, both nuclear and mitochondrial datasets reveal widespread historical fluctuations in population size (Figures 5 and 6). Similar cases have been documented in lizards (e.g., Myers et al. 2022), where geographic isolation, followed by range and demographic expansions, led to secondary contact and gene flow between previously diverged groups.

First, our divergence time estimates support a gradual and prolonged separation among species in the *Tropidurus spinulosus* group, with divergence events between species occurring from 20 Ma onward. Specifically, the initial split occurred between 20 and 15 Ma, with *T. melanopleurus* diverging first. Around 10 Ma, *T. callathelys* separated from the remaining taxa, while most subsequent speciation events took place between 8 and 2.5 Ma (Figure 3). Related to that, it is important to note that the evolutionary history of South America's dry diagonal has been shaped by multiple Neogene (23 Ma onward) geological and climatic processes, with individual taxa responding uniquely to local conditions (Guillory et al. 2024). Deep divergences among Squamates, including those within the *T. spinulosus* group, likely stem from Miocene events such as the uplift of the Central Brazilian Plateau and marine incursions in the southern dry diagonal (Guillory et al., 2024; Bezerra et al., 2025).

If such geological events led to prolonged geographic isolation of lineages, their gradual cessation would have increased opportunities for secondary contact and potential introgression, particularly when coupled with demographic and range expansions. In such a scenario, periods of secondary contact may have led to the formation of hybrid zones with varying levels of interbreeding, followed by contrasting patterns of gene flow between the nuclear and mitochondrial genomes. During periods of geographic and/or demographic expansion, nuclear genomes—subject to recombination and meiotic segregation—undergo widespread admixture and tend to homogenize over time, diluting distinct traces of past

isolation and secondary contact. In contrast, divergent mitochondrial haplotypes, which are non-recombining and inherited solely from the females, may persist due to genetic drift, particularly if introgression occurred early in the population expansion or when the population sizes were relatively low.

The directionality of gene flow events is another factor that could have played a crucial role in facilitating neutral mitochondrial capture. Because genetic drift is more pronounced in small populations, neutral mutations in mitogenomes are more likely to become fixed (Moore 1995; Després, 2019). Consequently, unidirectional introgression from a larger, resident population into a smaller, invading one would be more probable during the early stages of contact. If the ancestral populations of any of *Tropidurus spinulosus* species were more restricted in distribution at that point, such conditions would further facilitate the fixation of captured mitochondrial variants through drift. The repeated instances of discordance involving *T. xanthochilus*, due to ancient introgression, may suggest that this lineage had a smaller population size compared to others. Our ancestral population size estimates are consistent with this scenario. For instance, in the model where migration rates are higher (in this case, using the mitochondrial topology as the guide tree; Tables S3-S4), Θ estimates of *T. xanthochilus* are considerably lower than those of the ancestor involved in the gene flow event—in this case M (*T. xanthochilus*→ancestor (*T. guarani*, *T. spinulosus*)) = 0.3629, with Θ values of 0.0006258 and 0.02017, respectively (Table S5). A similar pattern was observed when the nuclear topology was used as the guide tree, with the ancestors of the *T. tarara* + *T. spinulosus* + *T. guarani* clade exhibiting higher Θ values than those of the ancestral *T. xanthochilus* populations (Table S6). Under this scenario, it would be plausible to suggest that the mitogenomes of some *T. xanthochilus* individuals could have been incorporated by the

larger ancestral populations of the *T. guarani* + *T. spinulosus* clade, and also by ancestral populations of *T. tarara*.

It is also noteworthy that our main demographic analyses (EBSP and Stairway Plot) might have captured a shorter time scale than that over which the gene flow events occurred. Even so, relatively recent demographic shifts, during the Pleistocene (2.5 Ma – 12 kya), may have contributed to the discordance pattern as well, either by facilitating the fixation of mitochondrial variants or reducing detectable signals of nuclear introgression. Population expansion events, in particular, appear to have occurred from at least 100 kya onward (Figures 5 and 6), supporting this interpretation. Similar patterns of demographic fluctuation shaping phylogeographic histories have been reported for other squamates as well (Guillory et al. 2024). Moreover, the observed differences in temporal estimates of species demography between those two approaches (Figures 5 and 6) are likely attributable to the distinct mutation rates we applied to the mitochondrial and nuclear datasets. As with many non-model organisms, species-specific substitution rate estimates for *Tropidurus* are unavailable, adding uncertainty to time-based inferences.

The two particular instances of mtDNA capture involving *Tropidurus xanthochilus* are also associated with biogeographic signals: one possibly occurring to the west of *T. xanthochilus*' distribution, involving ancestral populations of the *T. spinulosus + T. guarani* clade, and another to the south, involving *T. tarara*. Broadly speaking, *T. spinulosus* is found west of the Paraguay River, primarily within the Chaco region (Carvalho 2013). Specifically, its distribution spans from north-central Argentina and northwestern Paraguay to southeastern and central Bolivia, covering both the Chaco and dry forest zones (Frost et al. 1998; Carvalho 2013). Although distributional data remain limited, the known ranges of *T. spinulosus* and *T. xanthochilus* are allopatric. The nearest known populations of *T. spinulosus* are located at least

350 km south of the type locality of *T. xanthochilus,* near to the '*Serranía de Huanchaca*' (Harvey and Gutberlet, 1998). Even so, Harvey and Gutberlet (1998) proposed that *T. xanthochilus* and *T. spinulosus* might be parapatric in the area where the forests of the Tarvo and Paraguá Rivers merge with the semideciduous *'Chiquitania'* dry forest. On the other hand, *T. tarara* is currently documented from locations in the northern portion of Eastern Paraguay, east of the Paraguay River, and its range extends into the Brazilian state of Mato Grosso do Sul (near the southern limit of the distribution of *T. xanthochilus*).

In this context, future studies—whether empirical or based on modelling scenarios—will be crucial to assess the potential overlap (past or present) in the distributions of *T. xanthochilus* with *T. spinulosus* + *T. guarani* clade, and *T. tarara* as well. Such overlap would provide additional biogeographical evidence for mitochondrial capture among these lineages. Environmental changes can increase opportunities for hybridization and introgression through neutral demographic processes (Excoffier et al. 2009; Phuong et al. 2016), with mitonuclear discordance of this nature often linked to climatic instability and its effects on demographic dynamics (Phuong et al. 2016). Phylogenetic niche modeling, which combines past and present climate data with occurrence records and time-calibrated phylogenies to reconstruct historical geographic ranges (e.g., Guillory and Brown, 2021), may be particularly useful for testing these hypotheses in the future.

Finally, our findings suggest that mitochondrial capture in the *Tropidurus spinulosus* group likely occurred during a period when the current lineages were not yet fully differentiated and still overlapped in both space and time. This interpretation is supported by our migration rate results, which show that the highest estimated values were associated with scenarios involving ancestral populations (Figure 4). Particularly, this aligns with the "gray zone of speciation" concept—a transitional phase where populations shift from widespread

admixture to complete genetic isolation (Roux et al. 2016; Burbrink et al. 2021), facilitated by pre and/or post-zygotic barriers (Stankowski and Ravinet, 2021).

Mitonuclear discordance beyond neutral processes: a case for natural selection?

Our analyses did not reveal strong evidence of positive selection acting on the mitochondrial genome of the *Tropidurus spinulosus* species group. Site-model tests across the phylogeny identified only a few individual codons under selection, indicating that these methods captured limited signals of episodic or pervasive positive selection acting on the mitogenome. However, it is important to note that these approaches are designed to detect selection at the level of specific codons or phylogenetic branches, rather than to assess the rapid fixation of mitochondrial haplotypes following introgression (see the HyPhy documentation for a detailed explanation). In such a scenario, an entire haplotype could be fixed in a new species, a process that might not be directly detectable by the methods adopted here.

Nonetheless, complementary analyses, including nucleotide diversity estimates and Tajima's D test results, do not provide support for natural selection either. First, comparable π levels across the lineages involved in the discordance (Table S7) are not indicative of selective forces strongly acting on the mitogenomes of *Tropidurus spinulosus* species. Similarly, the negative Tajima's D values (Table S8), while theoretically compatible with both selection and population expansion, are here interpreted as indicative of historical demographic changes in light of the additional evidence previously discussed. Furthermore, in lizards—where mitochondrial function is less constrained by high metabolic demands compared to endotherms (Chung and Schulte 2020)—the selective pressure for rapid fixation of an introgressed mitogenome is likely lower. Nonetheless, while selective factors are unlikely

to be the primary drivers of mitonuclear discordance in *T. spinulosus* lineages, adaptive explanations may be still underrepresented in the literature (e.g., Mao and Rossiter 2020), which may partly reflect the inherent challenges in reliably detecting selection on mtDNA (Bonnet et al. 2017).

Sex-biased dispersal in Tropiduridae and its potential role in mitonuclear discordance

Finally, future investigations could look further into the role of mitonuclear incompatibilities and mating systems in explaining contrasting signals between nuDNA and mtDNA. Asymmetries between sexes in mating behavior, offspring production, and dispersal are well-known demographic factors contributing to mitonuclear discordance (Dessi et al. 2022). For example, in species where males exhibit greater dispersal, nuDNA is expected to show higher genetic homogeneity across distant populations, as male-mediated gene flow facilitates the spreading and mixing of their genetic material. Conversely, if females are more philopatric (i.e., remain near their birthplace), mtDNA may display greater population structure, preserving historical patterns of isolation. As a result, while nuDNA may indicate a single, cohesive population over a broad geographic range, mtDNA could reveal distinct subpopulations shaped by limited female dispersal. This process can lead to geographically structured mitochondrial lineages that persist despite widespread nuclear gene flow (see reviews in Toews and Brelsford 2012; Bonnet et al. 2017). Currently, empirical data on the dispersal behavior of *Tropidurus* species are lacking. However, research on certain groups closely related to Tropiduridae (e.g., Phrynosomatidae) suggest that females exhibit strong philopatry and possibly territoriality, while males may disperse further from contact zones, facilitating nuclear gene flow but limiting mitochondrial inheritance (Qi et al. 2013). Although limited studies have been conducted on squamate reptiles, some evidence indicates that sex-

biased differences in behavior and fitness can influence dispersal patterns. Therefore, we recommend future research to investigate whether sex-related dispersal contributes to the mitonuclear discordance observed in *Tropidurus*.

References

Allio R, et al. 2020. MitoFinder: Efficient automated large-scale extraction of mitogenomic data in target enrichment phylogenomics. Molecular Ecology Resources 20: 892-905.

Andersen MJ, et al. 2021. Complex histories of gene flow and a mitochondrial capture event in a non-sister pair of birds. Molecular Ecology 30: 2087–2103. https://doi.org/10.1111/mec.15856

Andrews S. 2010. FastQC: A Quality Control Tool for High Throughput Sequence Data [Online]. Available online at: http://www.bioinformatics.babraham.ac.uk/projects/fastqc/

Bankevich A, et al. 2012. SPAdes: a new genome assembly algorithm and its applications to single-cell sequencing. Journal of computational biology 19: 455-477.

Benavides E, Baum R, McClellan D, Sites Jr. JW. 2007. Molecular phylogenetics of the lizard genus *Microlophus* (Squamata: Tropiduridae): aligning and retrieving indel signals from nuclear introns. Systematic Biology 56: 776–797.

Benavides E, Baum R, Snell HM, Snell HL, Sites Jr JW. 2009. Island biogeography of Galápagos lava lizards (Tropiduridae: *Microlophus*): species diversity and colonization of the archipelago. Evolution 63: 1606–1626.

Bergeron LA, et al. 2023. Evolution of the germline mutation rate across vertebrates. Nature 615: 285-291.

Bezerra CH, et al. 2025. Biogeographical Origins of Caatinga Squamata Fauna. Journal of Biogeography 52: 521-531.

Bolger AM, Lohse M, Usadel B. 2014. Trimmomatic: a flexible trimmer for Illumina sequence data. Bioinformatics 30: 2114-2120.

Bonnet T, Leblois R, Rousset F, Crochet PA. 2017. A reassessment of explanations for discordant introgressions of mitochondrial and nuclear genomes. Evolution 71: 2140-2158.

Borowiec ML. 2016. AMAS: a fast tool for alignment manipulation and computing of summary statistics. PeerJ 4: e1660.

Bouckaert R, et al. 2019. BEAST 2.5: An advanced software platform for Bayesian evolutionary analysis. PLoS computational biology 15: e1006650.

Burbrink FT, Gehara M, McKelvy AD, Myers EA. 2021. Resolving spatial complexities of hybridization in the context of the gray zone of speciation in North American ratsnakes (*Pantherophis obsoletus* complex). Evolution 75: 260-277.

Bushnell B. 2018. BBTools: a suite of fast, multithreaded bioinformatics tools designed for analysis of DNA and RNA sequence data. *Joint Genome Institute*.

Cai R, Ané C. 2021. Assessing the fit of the multi-species network coalescent to multi-locus data. Bioinformatics 37: 634-641.

Camurugi F, et al. 2022. Isolation by distance and past climate resistance shaped the distribution of genealogical lineages of a neotropical lizard. Systematics and Biodiversity 20: 1-19.

Carvalho ALG. 2013. On the distribution and conservation of the South American lizard genus *Tropidurus* Wied-Neuwied, 1825 (Squamata: Tropiduridae). Zootaxa 3640: 42–56.

2016. Three New Species of the *Tropidurus spinulosus* Group (Squamata: Tropiduridae) from Eastern Paraguay. American Museum Novitates 3853: 1–44, doi:10.1206/3853.1

Carvalho ALG, de Britto MR, Fernandes DS. 2013. Biogeography of the Lizard Genus *Tropidurus* Wied-Neuwied, 1825 (Squamata: Tropiduridae): Distribution, Endemism, and Area Relationships in South America. PLoS One: 8.

Carvalho ALG, et al. 2016. A New *Tropidurus* (Tropiduridae) from the Semiarid Brazilian Caatinga: Evidence for Conflicting Signal between Mitochondrial and Nuclear Loci Affecting the Phylogenetic Reconstruction of South American Collared Lizards. American Museum Novitates 3852: 1–68.

Carvalho ALG, et al. 2024. A highly polymorphic South American collared lizard (Tropiduridae: *Tropidurus*) reveals that open–dry refugia from South-western Amazonia staged allopatric speciation. Zoological Journal of the Linnean Society 201: 493-533.

Castresana J. 2000. Selection of conserved blocks from multiple alignments for their use in phylogenetic analysis. Molecular biology and evolution 17: 540-552.

Chung DJ, Schulte PM. 2020. Mitochondria and the thermal limits of ectotherms. Journal of Experimental Biology 223: jeb227801.

Clement M, Snell Q, Walke P, Posada D, Crandall K. 2002. TCS: estimating gene genealogies. In *Parallel and distributed processing symposium, international* (Vol. 2, pp. 7-pp). IEEE Computer Society.

DeRaad DA. 2022. SNPfiltR: an R package for interactive and reproducible SNP filtering. Molecular Ecology Resources 22: 2443-2453.

DeRaad DA, et al. 2023. Mitonuclear discordance results from incomplete lineage sorting, with no detectable evidence for gene flow, in a rapid radiation of *Todiramphus* kingfishers. Molecular Ecology 32: 4844–4862. https://doi.org/10.1111/mec.17080

Després L. 2019. One, two or more species? Mitonuclear discordance and species delimitation. Molecular Ecology 28: 3845–3847. https://doi.org/10.1111/mec.15211

Dessi MC, et al. 2022. The role of sex-biased dispersion in promoting mitonuclear discordance in *Partamona helleri* (Hymenoptera: Apidae: Meliponini). Biological Journal of the Linnean Society 136: 423-435.

Dong X, et al. 2023. Mitochondrial introgression and mito-nuclear discordance obscured the closely related species boundaries in Cletus Stål from China (Heteroptera: Coreidae). Molecular Phylogenetics and Evolution 184. https://doi.org/10.1016/j.ympev.2023.107802

Dufresnes C, et al. 2020. Are glacial refugia hotspots of speciation and cytonuclear discordances? Answers from the genomic phylogeography of Spanish common frogs. Molecular Ecology 29: 986–1000. https://doi.org/10.1111/mec.15368

Durand EY, Patterson N, Reich D, Slatkin M. 2011. Testing for ancient admixture between closely related populations. Molecular Biology and Evolution 28: 2239-2252.

Excoffier L, Foll M, Petit RJ. 2009. Genetic consequences of range expansions. Annual Review of Ecology, Evolution, and Systematics 40: 481-501.

Faircloth BC, et al. 2012. Ultraconserved elements anchor thousands of genetic markers spanning multiple evolutionary timescales. Systematic Biology 61: 717-26.

Faircloth BC. 2016. PHYLUCE is a software package for the analysis of conserved genomic loci. Bioinformatics 32: 786–788.

Fedorov VB, Trucchi E, Goropashnaya AV, Stenseth NC. 2022. Conflicting nuclear and mitogenome phylogenies reveal ancient mitochondrial replacement between two North American species of collared lemmings (*Dicrostonyx groenlandicus*, *D. hudsonius*). Molecular phylogenetics and evolution 168.

Firneno TJ, et al. 2021. Delimitation despite discordance: Evaluating the species limits of a confounding species complex in the face of mitonuclear discordance. Ecology and Evolution 11: 12739–12753. https://doi.org/10.1002/ece3.8018

Flouri T, Jiao X, Rannala B, Yang Z. 2018. Species Tree Inference with BPP using Genomic Sequences and the Multispecies Coalescent. Molecular Biology and Evolution 35: 2585-2593. doi:10.1093/molbev/msy147

Flouri T, Jiao X, Huang J, Rannala B, Yang Z. 2023. Efficient Bayesian inference under the multispecies coalescent with migration. Proceedings of the National Academy of Sciences 120: e2310708120.

Frost DR, Crafts HM, Fitzgerald LA, Titus TA. 1998. Geographic variation, species recognition, and molecular evolution of cytochrome oxidase I in the *Tropidurus spinulosus* complex (Iguania: Tropiduridae). Copeia: 839-851.

Good JM, Vanderpool D, Keeble S, Bi K. 2015. Negligible nuclear introgression despite complete mitochondrial capture between two species of chipmunks. Evolution 69: 1961–1972. https://doi.org/10.1111/evo.12712

Guillory WX, Brown JL. 2021. A new method for integrating ecological niche modeling with phylogenetics to estimate ancestral distributions. Systematic Biology 70: 1033-1045.

Guillory WX, et al. 2024. Geoclimatic drivers of diversification in the largest arid and semi-arid environment of the Neotropics: Perspectives from phylogeography. Molecular Ecology e17431.

Gutenkunst RN, Hernandez RD, Williamson SH, Bustamante CD. 2009. Inferring the joint demographic history of multiple populations from multidimensional SNP data. PLoS Genetics, 5:e1000695

Harris RS. 2007. *Improved pairwise alignment of genomic DNA*. The Pennsylvania State University.

Harvey MB, Gutberlet Jr RL. 1998. Lizards of the genus *Tropidurus* (Iguania: Tropiduridae) from the Serranía de Huanchaca, Bolivia: new species, natural history, and a key to the genus. Herpetologica 493-520.

Harvey MG, Smith BT, Glenn TC, Faircloth BC, Brumfield RT. 2016. Sequence capture versus restriction site associated DNA sequencing for shallow systematics. Systematic Biology 65: 910-924.

Heled J, Drummond AJ. 2008. Bayesian inference of population size history from multiple loci. BMC evolutionary biology 8: 1-15.

Hibbins MS, Hahn MW. 2022. Phylogenomic approaches to detecting and characterizing introgression. Genetics 220.

Hinojosa JC, et al. 2019. A mirage of cryptic species: Genomics uncover striking mitonuclear discordance in the butterfly *Thymelicus sylvestris*. Molecular Ecology 28: 3857–3868. https://doi.org/10.1111/mec.15153

Kalyaanamoorthy S, Minh BQ, Wong TK, Von Haeseler A, Jermiin LS. 2017. ModelFinder: fast model selection for accurate phylogenetic estimates. Nature methods 14: 587-589.

Katoh K, Standley DM. 2013. MAFFT multiple sequence alignment software version 7: improvements in performance and usability. Molecular biology and evolution 30: 772-780.

Knaus BJ, Grünwald NJ. 2017. vcfr: a package to manipulate and visualize variant call format data in R. Molecular Ecology Resources 17: 44-53.

Leigh JW, Bryant D, Nakagawa S. 2015. POPART: full-feature software for haplotype network construction. Methods in Ecology & Evolution 6.

Li H, et al. 2009. The sequence alignment/map format and SAMtools. Bioinformatics 25: 2078-2079.

Li H. 2013. Aligning sequence reads, clone sequences and assembly contigs with BWA-MEM. arXiv:1303.3997v2 [q-bio.GN].

Liu X, Fu YX. 2020. Stairway Plot 2: demographic history inference with folded SNP frequency spectra. Genome biology 21: 280.

Lutteropp S, Scornavacca C, Kozlov AM, Morel B, Stamatakis A. 2022. NetRAX: accurate and fast maximum likelihood phylogenetic network inference. Bioinformatics 38: 3725-3733.

Malinsky M, Matschiner M, Svardal H. 2021. Dsuite-Fast D-statistics and related admixture evidence from VCF files. Molecular ecology resources 21: 584-595.

Mao X, Rossiter SJ. 2020. Genome-wide data reveal discordant mitonuclear introgression in the intermediate horseshoe bat (*Rhinolophus affinis*). Molecular phylogenetics and evolution, 150: 106886.

McKenna A, et al. 2010. The Genome Analysis Toolkit: a MapReduce framework for analyzing next-generation DNA sequencing data. Genome research 20: 1297-1303.

Minh BQ, et al. 2020. IQ-TREE 2: new models and efficient methods for phylogenetic inference in the genomic era. Molecular biology and evolution 37: 1530-1534.

Moore WS. 1995. Inferring phylogenies from mtDNA variation: mitochondrial-gene trees versus nuclear-gene trees. Evolution 49: 718-726.

Murrell B, et al. 2012. Detecting individual sites subject to episodic diversifying selection. PLoS genetics 8: e1002764.

Murrell B, et al. 2013. FUBAR: a fast, unconstrained bayesian approximation for inferring selection. Molecular biology and evolution 30: 1196-1205.

Murrell B, et al. 2015. Gene-wide identification of episodic selection. Molecular biology and evolution 32: 1365-1371.

Myers EA, et al. 2022. Interspecific gene flow and mitochondrial genome capture during the radiation of Jamaican *Anolis* lizards (Squamata: Iguanidae). Systematic Biology 71: 501-511.

Olson DM, et al. 2001. Terrestrial ecoregions of the world: a new map of life on Earth. BioScience 51: 933–938.

Palacios C, Campagna L, Parra JL,Cadena CD. 2023. Mito-nuclear discordance in the phenotypically variable Andean hummingbirds *Coeligena bonapartei* and *Coeligena helianthea* (Trochilidae). Biological Journal of the Linnean Society 139: 145-157.

Paradis E. 2010. pegas: an R package for population genetics with an integrated–modular approach. Bioinformatics 26: 419-420.

Phuong MA, Bi K, Moritz C. 2016. Range instability leads to cytonuclear discordance in a morphologically cryptic ground squirrel species complex. Molecular Ecology 26: 4743–4755. https://doi.org/10.1111/mec.14238

Purcell S, et al. 2007. PLINK: a tool set for whole-genome association and population-based linkage analyses. The American journal of human genetics 81: 559-575.

Qi Y, Yang W, Lu B, Fu J. 2013. Genetic evidence for male-biased dispersal in the Qinghai toad-headed agamid *Phrynocephalus vlangalii* and its potential link to individual social interactions. Ecology & Evolution 3: 1219-1230.

Rambaut A, Drummond AJ. 2014. LogCombiner v2. 1.3. Edinburgh (UK): Institute of Evolutionary Biology, University of Edinburgh.

Rambaut A. 2014. FigTree v.1.4.2: tree drawing tool. Available at: http://tree.bio.ed.ac.uk/software/figtree/

Rambaut A, Drummond AJ, Xi D, Baele G, Suchard MA. 2018. Posterior summarization in Bayesian phylogenetics using Tracer 1.7. Systematic biology 67: 901-904.

Rancilhac L, et al. 2021. Phylotranscriptomic evidence for pervasive ancient hybridization among Old World salamanders. Molecular Phylogenetics and Evolution, 155. https://doi.org/10.1016/j.ympev.2020.106967

Raposo do Amaral F, et al. 2018. Recent chapters of Neotropical history overlooked in phylogeography: Shallow divergence explains phenotype and genotype uncoupling in *Antilophia* manakins. Molecular ecology 27: 4108-4120.

dos Reis M, Yang Z. 2019. Bayesian molecular clock dating using genome-scale datasets. *Evolutionary genomics: Statistical and computational methods*, 309-330.

Roux C, et al. 2016. Shedding light on the grey zone of speciation along a continuum of genomic divergence. PLoS biology 14.

Seixas FA, Boursot P, Melo-Ferreira J. 2018. The genomic impact of historical hybridization with massive mitochondrial DNA introgression. Genome Biology 19. https://doi.org/10.1186/s13059-018-1471-8

Shen CC, Miura I, Lin TH, Toda M, Nguyen HN, Tseng HY, & Lin SM. 2025. Exploring Mitonuclear Discordance: Ghost Introgression From an Ancient Extinction Lineage in the *Odorrana swinhoana* Complex. Molecular Ecology e17763.

Smith BT, Harvey MG, Faircloth BC, Glenn TC, Brumfield RT. 2014. Target Capture and Massively Parallel Sequencing of Ultraconserved Elements (UCEs) for Comparative Studies at Shallow Evolutionary Time Scales. Syst Biol 64: 83-95. doi:10.1093/sysbio/syt061.

Smith MD, et al. 2015. Less is more: an adaptive branch-site random effects model for efficient detection of episodic diversifying selection. Molecular biology and evolution 32: 1342-1353.

Smith SA, Brown JW, Walker JF. 2018. So many genes, so little time: a practical approach to divergence-time estimation in the genomic era. PloS one 13: e0197433.

Solís-Lemus C, Ané C. 2016. Inferring phylogenetic networks with maximum pseudolikelihood under incomplete lineage sorting. PLoS genetics 12: e1005896.

Solís-Lemus C, Yang M, Ané C. 2016. Inconsistency of species tree methods under gene flow. Systematic biology 65: 843-851.

Solís-Lemus C, Bastide P, Ané C. 2017. PhyloNetworks: a package for phylogenetic networks. Molecular biology and evolution 34: 3292-3298.

Stankowski S, Ravinet M. 2021. Defining the speciation continuum. Evolution 75: 1256-1273.

Tamura K, Qiqing T, Kumar S. 2018. Theoretical Foundation of the RelTime Method for Estimating Divergence Times from Variable Evolutionary Rates. Molecular Biology and Evolution 35: 1770-1782.

Tamura K, Stecher G, Kumar S. 2021. MEGA 11: Molecular Evolutionary Genetics Analysis Version 11. Molecular Biology and Evolution. https://doi.org/10.1093/molbev/msab120.

Tao Q, Tamura K. Mello B, Kumar S. 2020. Reliable Confidence Intervals for RelTime Estimates of Evolutionary Divergence Times. Molecular Biology and Evolution 37: 280-290.

Toews DP, Brelsford A. 2012. The biogeography of mitochondrial and nuclear discordance in animals. Molecular ecology 21: 3907-3930.

Wen D, Yu Y, Zhu J, Nakhleh L. 2018. Inferring phylogenetic networks using PhyloNet. Systematic biology 67: 735-740.

Werneck FP, Leite RN, Geurgas SR, Rodrigues MT. 2015. Biogeographic history and cryptic diversity of saxicolous Tropiduridae lizards endemic to the semiarid Caatinga. BMC Evolutionary Biology 15: 1-24.

Zarza E, et al. 2016. Hidden histories of gene flow in highland birds revealed with genomic markers. Molecular Ecology, 25: 5144-5157.

Zhang C, Rabiee M, Sayyari E, Mirarab S. 2018. ASTRAL-III: polynomial time species tree reconstruction from partially resolved gene trees. BMC bioinformatics 19: 15-30.

Zheng Y, Wiens JJ. 2016. Combining phylogenomic and supermatrix approaches, and a time-calibrated phylogeny for squamate reptiles (lizards and snakes) based on 52 genes and 4162 species. Molecular phylogenetics and evolution 94: 537-547.

Zieliński P, et al. 2013. No evidence for nuclear introgression despite complete mtDNA replacement in the Carpathian newt (*Lissotriton montandoni*). Molecular Ecology 22: 1884-1903.